Journal of Hazardous Materials, 14 (1987) 365–386
Elsevier Science Publishers B.V., Amsterdam — Printed in The Netherlands

DISCHARGE OF CONDENSED SULFUR DIOXIDE: A FIELD TEST STUDY OF THE SOURCE BEHAVIOUR WITH DIFFERENT RELEASE GEOMETRIES

K. NYREN and S. WINTER

National Defence Research Institute, Department 4, S-90182 Umeå (Sweden)

(Received February 20, 1986; accepted in revised form August 28, 1986)

Summary

The physical factors determining the mass flow rate, early dilution and the tendency to form ground deposits were studied by discharging condensed sulfur dioxide from a pressure vessel through a hole and a pipe, respectively. The results indicate that ground deposits do not easily arise and that the liquid phase evaporates very quickly. In the pipe releases, the mass flow rate was strongly dependent on the thermodynamic state in the vessel. Even a moderate excess pressure (compared to the saturation pressure) in the vessel increased the mass flow rate markedly. A theoretical model for two-phase release through ducts which agrees well with the pipe tests is also presented. In the aperture releases two-phase phenomena did not affect the mass flow rate and thus the Bernoulli formula for incompressible outflow was valid. Substantial extra air entrainment occurred near the exhaust opening because of the radial momentum produced by a vigorous flash.

1 Introduction

The source behaviour could be of vital importance both to short and long range hazards posed to people when a condensed pressurized gas is discharged to the atomosphere from the liquid space of a storage vessel. The consequences of this kind of release are, however, difficult to predict because of the complexity of the physical phenomena.

One of the difficulties is to predict the mass flow rate. Different assumptions of how and when the liquid flashes (rapid partial evaporation) will greatly influence the calculation of the mass flow. The release geometry as well as the thermodynamic state in the vessel are of vital importance here.

Another uncertainty is the possibility of rain-out or impaction of a fraction of the liquid, e.g. if liquid sulfur dioxide at 15°C is discharged to the atmosphere, it is theoretically possible that 90% of the gas (all of the liquid phase left after the flash) could accumulate on the ground. The real figure depends, among other things, on the breakup of the liquid phase into drops and the rate of air entrainment into the momentum jet.

If the gas is inflammable, the early dilution will become important. With

0304-3894/87/$03.50

different assumptions on where (and how fast) the flashing process is supposed to start many different mass flow rates and momentum flow rates are possible. This means that prediction of fire hazards becomes very uncertain.

Good data from full-scale experiments are scarce. One test series with hazardous gas allowing some conclusions are the field experiments with ammonia in Landskrona, Sweden, 1983 [1]. In these tests pressurized saturated ammonia was released from the liquid phase through a pipe. It was found that the mass flow was considerably reduced because of flash in the pipe. Moreover the air entrainment into the jet was efficient (due to the overpressure at the outlet which accelerates the flow) and no accumulation of liquid on the ground occurred. Yet these experiments do not answer all the vital questions.

One question is what happens if the thermodynamic pressure energy is substantially smaller than in the ammonia experiments. Will that give rise to a more delayed flash associated with a less efficient damping of the mass flow in a pipe break situation? Does important ground accumulation occur? Another important question is whether a hole directly in the tank wall is associated with any hazard-limiting choked-flow mechanism.

In this paper we report the results and interpretation of field experiments with release of sulfur dioxide from a pressure vessel. The aims of the tests were:

(a) To measure the mass flow rate, the state in the vessel, and the jet-determining parameters when the gas is released from the liquid space of a pressure vessel. This is done with a duct configuration (straight pipe) as well as an aperture configuration.

(b) To measure the fraction of the released gas reaching the ground as a liquid and to find out whether bunds for liquid collection are effective or not for a pressurized gas with a relatively small thermodynamic pressure energy.

(c) To find ways of predicting the source behaviour by the aid of physically reasonable mathematical modelling.

Finally, it should be mentioned that the main reason for choosing pressurized sulfur dioxide as a test substance was that it is stored and transported in large quantities in Sweden (as well as in many other countries).

2 Experiments

2.1 Apparatus

Figure 1 shows the basic apparatus, consisting of modified 2.6 m^3 commercial storage tank. The tank was modified to allow the study of almost any kind of release geometry in a simple and repeatable way. This equipment makes it possible to simulate "perforated tank wall" in a controllable manner. The design consisted of a short horizontal duct from the bottom part of the tank. This duct was much wider than the release openings and consisted mainly of a large valve. A flange with the desired release geometry could then be attached in front of the short and wide channel.

Fig. 1. The test tank in operation. The valve is operated manually to achieve short opening and closing times.

The two release geometries used in this work are shown in Figs. 2–4. The intention with this choice was to approximate experimentally situations with accidental pipe break or tank perforation.

The temperature of the tank liquid was measured with a thermocouple attached to the tank wall. A special paste was used to ensure good thermal contact. A thick layer of foam plastic also covered the contact point to avoid thermal contact with the environment. Temperatures at other places near the tank were measured by two mobile thermocouples.

The tank pressure was measured by using a Bofors TDS-1 absolute pressure transducer (range: 0–25 bar, precision: 0.05 bar) and amplifier, connected to the vapour space of the tank.

Another pressure transducer of the same kind was connected to the pipe end (see Fig. 2) via a hole of 3 mm bore in the pipe wall. The pressure transducers were calibrated on site shortly before each release by the aid of a precision manometer attached to a small test tank.

The tank weight was determined with four load cells whose signals were added together into one single analogue signal. The precision of this balance equipment was about 1 kg.

All analogue voltage signals (weight, pressure, temperature) were collected

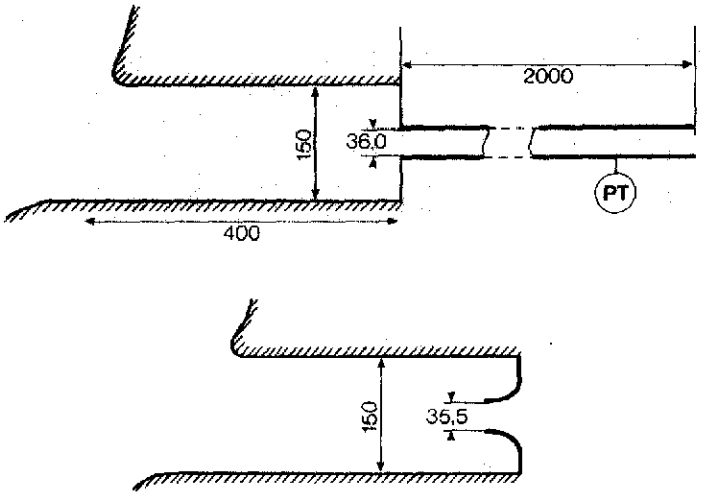

Fig. 2. Inner profiles of the two release sections. Part of the wide channel is a large valve for release control. Hatched lines are schematic and do not show exact detail. PT is a pressure tap.

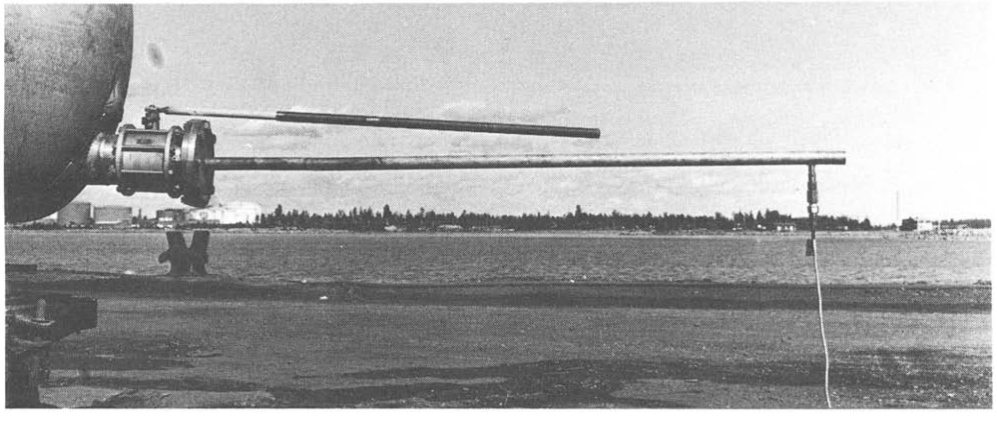

Fig. 3. The pipe configuration. The lever above the pipe is for manual control of the release valve.

and digitized by a Declab-03 computer system operating at a sampling frequency of 10 Hz.

Two 35 mm cameras, a 16 mm motion picture camera and a video camera were used to record the releases visually. The movie films were also used to determine release duration in some cases.

2.2 Methods of operation and handling of data

The release valve was operated manually. This means, opening and closing times could be reduced to 0.5 s. All releases were made in a similar manner and below we list how physical data were collected and handled in each release trial.

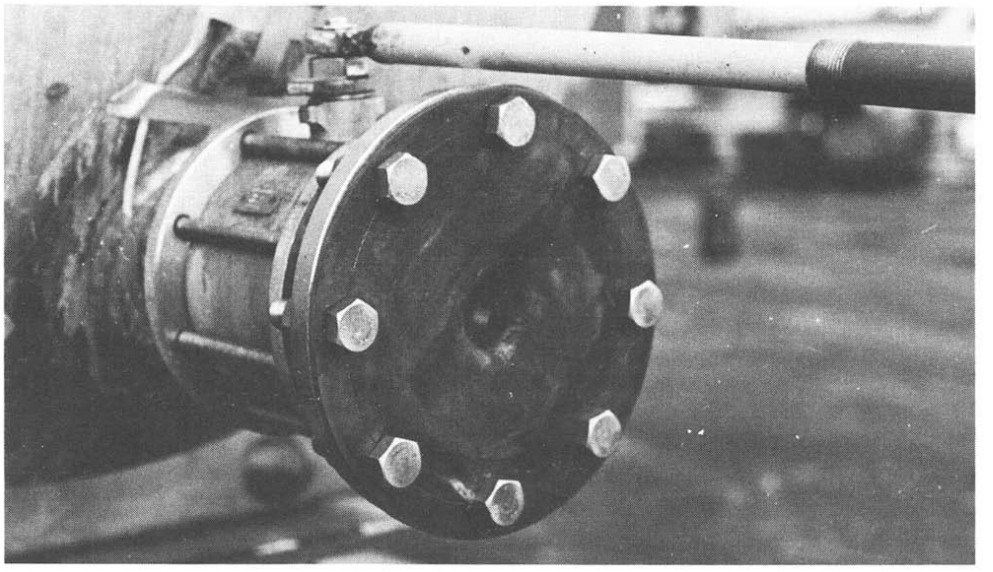

Fig. 4. Close-up of the aperture configuration.

- The two pressure signals (tank pressure and pipe exit pressure) were calibrated against the manometer shortly before each release. This was done at 1.00 bar and 4.00 bar, respectively. This procedure was necessary because of a slow signal deviation of about 0.10 bar/h. The pressure recording started at least a few seconds before the valve was opened and continued until about one minute after the valve was closed. Ten readings per second were collected. To eliminates insignificant high-frequency noise the signal was filtered using a moving-average procedure with 0.50 s window width.
- The tank weight signal was recorded in the same way as the pressures. This signal was also read manually before and after the release. The signal obtained during the release could not be used as expected because the manual valve operations and the jet thrust caused too large perturbations. This means that the mass flow rate could not be determined as a function of time. On the other hand a good average for the whole release time was obtained.
- As transient mass flow rates were not measured successfully it was necessary to determine the duration of each release carefully. This was automatically achieved in the pipe releases since the pipe exit pressure changed abruptly when the valve opened or closed. The release duration of the aperture releases was determined by recording the release jet with a 16 mm movie camera (25 exposures/s). The start time of all releases was defined to be exactly in the middle of the time interval during which the valve opened. The release stop time was defined analogously.

- The wind direction and the wind speed were measured by simple methods. This was done mainly for safety reasons. Also air humidity, temperature, and pressure were recorded in connection with each release.

2.3 External test conditions

The trials took place on the eastern shore of the Boliden Metall. Co. smelting plant (Skelleftehamn, Sweden) in August 1984. This site was preferred because of the availability of industrial emergency personnel specially trained to handle the technical and medical problems associated with toxic-gas releases.

The sector of preferred wind directions was uncomfortably narrow because of some populated islands in the vicinity of the release point. Because of this, the discharges were limited to 500 kg, which unfortunately restricted the release durations considerably.

To further limit the possible consequences of wind changes the cloud visibility was enhanced by injecting ammonia vapour (10 g/s, 30 m downwind of the tank) into the plume of sulphur dioxide as an efficient way of keeping track of the cloud over long distances.

Despite the trial limitation six releases could be carried out during the scheduled test week. Favourable wind conditions prevailed during two consecutive mornings allowing for three pipe releases and three aperture releases. Unfortunately, further tests to achieve more parameter variations or to correct for experimental mishaps were not possible.

One mishap was, e.g., the second test where the time interval between calibration of the pressure transducers and the release became far too long due to the appearance of a boat in the hazard sector. Therefore, this test had to be excluded from the data evaluation.

The most unfortunate experimental mishap was undoubtedly the temperature measurements in the release jet and on the ground in front of the release opening. It turned out that the vapour–aerosol–air mixture approached equilibrium much faster than expected and that the range of the thermometers was insufficient. They rapidly reached their bottom value $-25.5\,^{\circ}C$. Unfortunately, there was no possibility to rebuild the thermometer amplifiers on site due to the restricted periods of useful wind directions.

3 Experimental results and model comparisons

Six release trials were performed. The first three (P1, P2 and P3) with the pipe attached and then three (A1, A2 and A3) with the aperture attached. Because of the uncertainty with the pressure readings, P2 was disregarded from data evaluation. The tank was filled before P1 and was refilled before P3. The fillings were made well in advance of the releases (more than 10 h) to allow for the tank contents to reach equilibrium with the surroundings.

Three theoretical models were used in the evaluation of the collected data. The models (simply called model 1, 2 and 3) are described in the Appendix.

3.1 Mass flow rates and tank conditions for the pipe releases

The time–pressure history for P1 and P3 is shown in Figs. 5 and 6. The humps in one of the tank pressure curves are caused by a bad contact in the power supply to the transducer amplifier and do not reflect real pressure variations. The tank weight signal had corresponding and very clearly defined humps. This allowed for an exact determination of the time intervals not to be considered in P1.

The circles in Figs. 5 and 6 are theoretical exit pressures obtained with a two-phase model (See the Appendix, model 1) with the experimental tank pressures and tank temperatures as input. The tank pressures used in these calculations are averages from six-second time intervals centered around each point of time. Exceptions are a couple of points in trial P1 which are based on shorter intervals because of the power supply errors.

The tank liquid temperature was almost constant during the releases. Furthermore, the temperature remained unaltered during the minutes following each release. Thus the constancy of the temperature signal during the release is not due to slow thermal conduction through the tank wall but reflects a real physical state of the tank liquid. The measured tank liquid temperatures are given in the figure captions.

Two things are evident from the pressure curves:

(a) The tank liquid is not in equilibrium with the vapour in the tank. It is obviously subcooled (or overpressurized). This subcooling, however, decreases during the release when the vapour space of the vessel expands.

(b) Within eperimental error, the pipe exit pressure agrees with the saturation pressure for the tank liquid. This is exactly what should happen according to model 1 if the subcooling exceeds a certain level (see section 4 and the Appendix).

The subcooling of the tank liquid, which occured in all tests, could be explained by solar radiation heating the gas bubble above the liquid.

In Table 1, measured average mass flow rates are compared to calculated rates for the pipe releases. The perturbed intervals (see Fig. 5) in the tank pressure curve for the trial P1 were replaced with straight line portions to obtain the mass flow rates M1 and M2.

An immediate observation from Table 1 is that the fluid remains liquid throughout the pipe although the pressure at the exit is above atmospheric (choked flow). This is contrary to normal expectations for a choked flow and is obviously caused by the subcooled state of the tank liquid. Note that this phenomenon is not at all related to delayed flash (i.e. that the liquid is super-

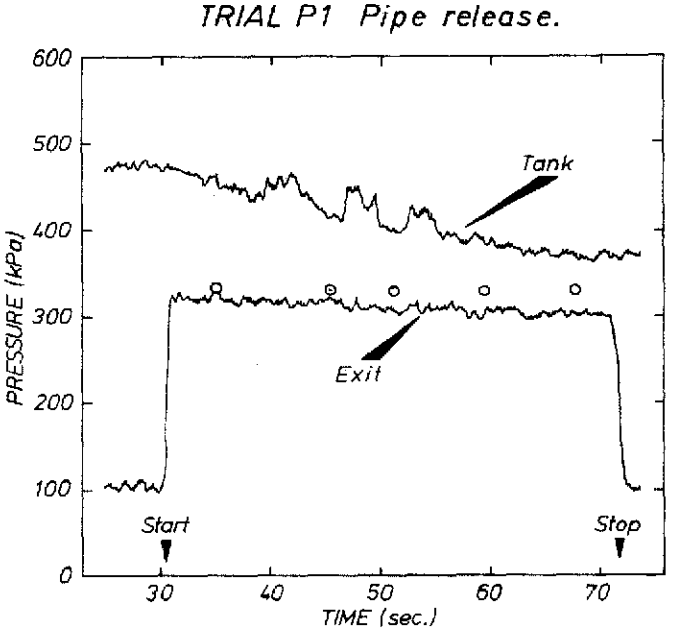

Fig. 5. Tank pressure and pipe exit pressure for trial P1 (the three humps in the upper curve are caused by a loss of power supply). The measured temperature of the tank liquid was 19.9°C corresponding to a saturation pressure of 329 kPa. The circles are exit pressures according to model 1 (see the Appendix) with the measured tank pressure and tank temperature as inputs.

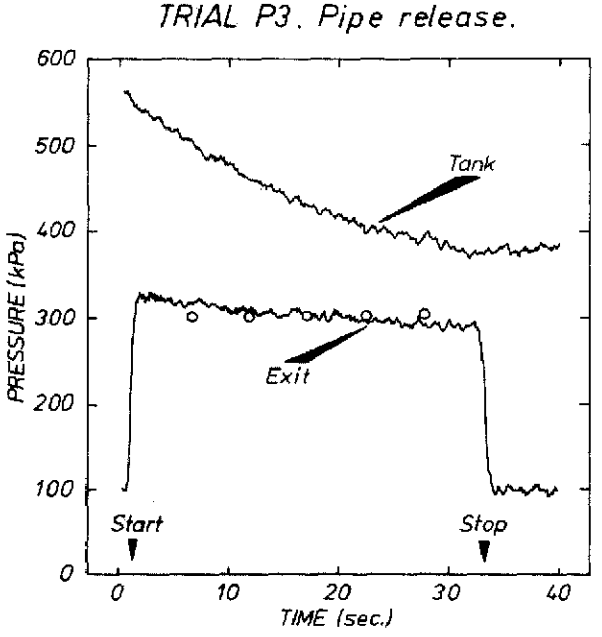

Fig. 6. Tank pressure and pipe exit pressure for trial P3. The tank liquid temperature was 17.2°C corresponding to a saturation pressure of 301 kPa. The circles have the same meaning as in Fig. 5.

TABLE 1

Time averaged mass flow rates (kg/s) for the pipe releases

Trial no.	ME[a]	M1[b]	M2[c]
P1	10.5	9.2	10.3
P2	8.9	[d]	[d]
P3	12.0	12.3	12.2

[a]ME = experimental rate.
[b]M1 = rate according to model 1 (a two-phase model) where the measured tank pressure and tank temperature were used as input.
[c]M2 = rate according to model 2 (a liquid-release model) where both the measured pressures were used as input. The models are described in the Appendix.
[d]Excluded due to missed pressure registrations.

heated in the pipe). The exit pressure measurements (Figs. 5 and 6) show that the liquid is approximately at its boiling point when it reaches the pipe end.

Also notice that the two-phase model (model 1) correctly predicts this behaviour. It gives a pure liquid flow in the pipe, an accurate exit pressure, and an accurate mass flow rate when using the measured tank conditions as input. The model calculations also show that the mass flow rate is very sensitive to the degree of subcooling. This aspect is further discussed in section 4.

3.2 Mass flow rates and tank conditions for the aperture releases

The tank pressure histories for the aperture discharges A1, A2 and A3 are shown in Fig. 7. The results are analogous to those for the pipe. The temperature remains constant while the excess pressure decreases towards equilibrium. Although no attempts were made to measure the pressure in the exhaust hole, there are strong reasons to believe that the increased exit pressure observed in the pipe releases does not occur here. This is seen in Table 2 where time-averaged mass flow rates are shown. A good theoretical fit (using the Bernoulli liquid–flow equation) is clearly obtained, if the exit pressure equals the atmospheric back pressure.

The conclusion is that the short exhaust channel allows the fluid to leave the hole as a superheated liquid jet which flashes outside the hole without enhancing the exit pressure.

3.3 The turbulent jet and the ground deposits

Since the fluid is (or becomes) a superheated liquid when it leaves the exit opening a vigorous flash forming a turbulent spray jet is to be expected. The reason for this is the considerable amount of energy (about 2 kJ/kg in these tests) released when the fluid expands adiabatically to atmospheric pressure.

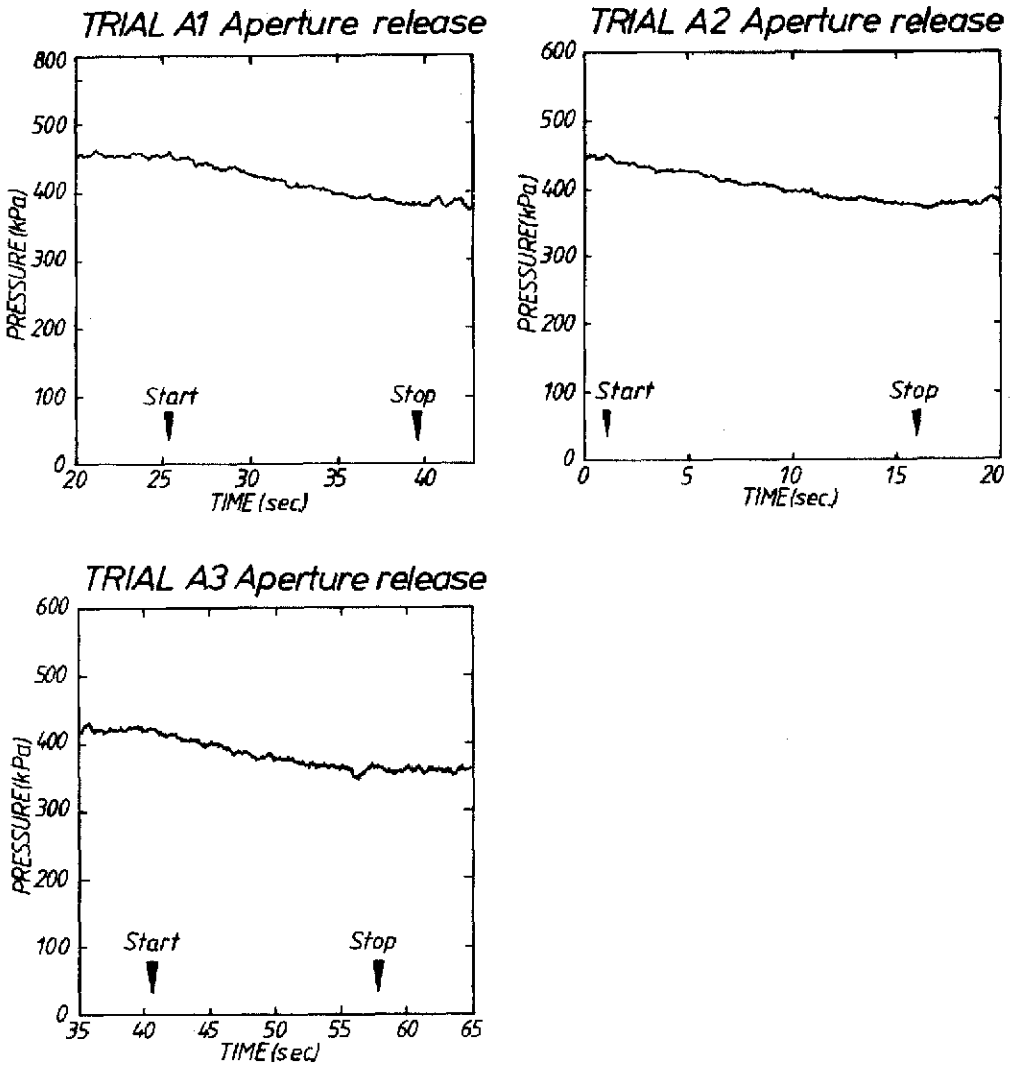

Fig. 7. Tank pressure versus time for the aperture releases. The tank liquid temperatures were 18.3°C, 18.2°C, and 17.4°C in trials A1, A2, and A3, respectively.

The experimental observations are consistent with these expectations. Figs. 8 and 9 show lateral views of the jet for a pipe release and an aperture release, respectively.

Due to the sudden flash, the jet diameter increases substantially just beyond the opening, whereafter "normal" jet mechanisms take over. Furthermore, there were no signs of rain-out from the jet in agreement with the visual impression of "steam".

Another observation was that the aperture jets had a bigger angle of expansion than the pipe jets. The reason for this is probably that the pipe jet achieves

TABLE 2

Time-averaged mass flow rates (kg/s) for the aperture releases

Trial no.	ME[a]	M3[b]
A1	14.0	14.6
A2	14.1	14.4
A3	13.2	13.9

[a]ME = experimental rate.
[b]M3 = rate according to model 3 (a liquid-flow model) using the measured tank pressure and the atmospheric pressure as exit pressure.

a higher momentum flux (in relation to the mass flow) due to the increased exit pressure which accelerates the fluid after the exit opening.

In trials P3, A1, A2, and A3 the temperature was recorded on the jet axis 1.80 m from the release opening. As mentioned before these measurements failed due to the unexpectedly fast evaporation of the liquid phase which caused the temperature to fall below the thermometer range. Anyhow it is possible to derive from the temperature curves (see Fig. 10) that the temperature could have been as low as $-40\,^{\circ}C$.

It was planned to measure the amount of liquid reaching the ground with a specially designed collecting device. This could not be done for the simple reason that no signs of collectable liquid deposits could be observed at all. Only a thin layer of condensed air humidity (water ice) with a smell of the gas could be observed on the ground after the releases. These ice deposits looked the same in all trials with an elliptical chape extending from the release hole to about 12–15 m away. The width was about 3 m. In Fig. 11 is shown what the deposits looked like after a release. The temperature of these deposits was well below the thermometer bottom range of $-25\,^{\circ}C$ in the same way as for the jet temperature.

4 Discussion

4.1 The influence of subcooled tank liquid on a pipe release

In these tests the tank liquid was markedly subcooled prior to each release although the tank fillings were made well in advance. The pressure curves (Figs. 5 and 6) also show that the overpressure decays gradually towards equilibrium when the gas space above the liquid expands during a release. This decay rate is of course directly dependent on the ratio of release hole area to tank volume. Knowledge about the impact of overpressure on hazards therefore becomes of interest as soon as a storage vessel is large enough to allow for a subcooled state to persist for a longer time period. The possibility of perma-

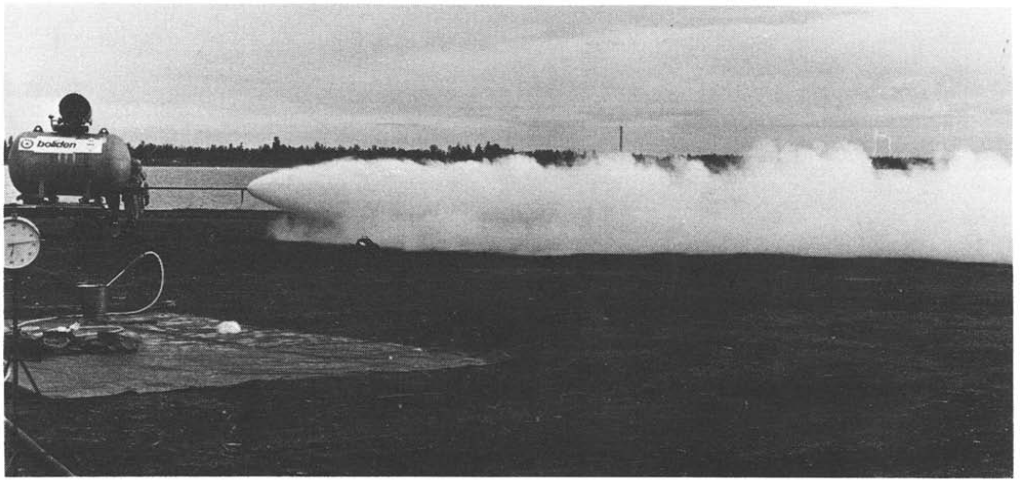

Fig. 8. Turbulent jet from trial P3 about five seconds after the release started. The tank is 2.8 m long for size reference. The wind speed is about 2 m/s directed along the jet axis. The relative humidity and temperature of the ambient air were 77% and 15°C, respectively.

Fig. 9. Turbulent jet from trial A3 about five seconds after the release started. The wind speed is about 2–3 m/s along the jet axis. The relative humidity and temperature of the ambient air were 68% and 19°C, respectively.

nent overpressure should also be borne in mind, e.g. hydrostatic liquid column pressure at the bottom of vessels of considerable height.

The first question is how various degrees of subcooling affects the mass flow rate. Our experiments with sulfur dioxide do not answer the question directly because the mass flow rate was recorded as an average. Moreover, the release durations were too short in order to reach saturation pressure in the tank.

It is, however, possible to predict quite accurately the mass flow rate at lower

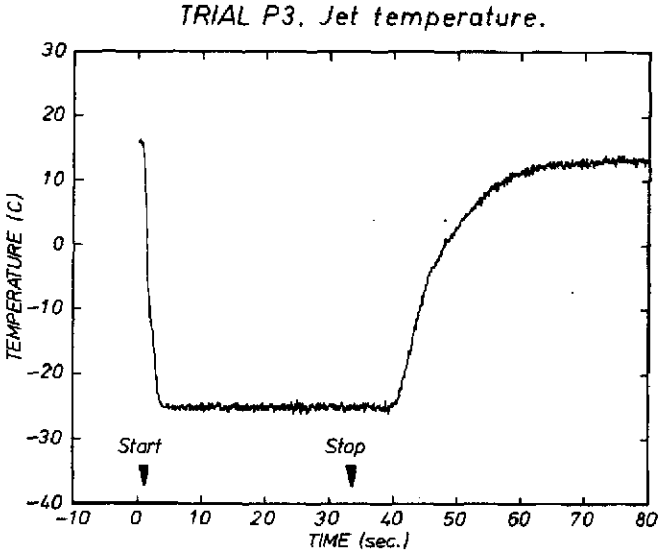

Fig. 10. One of the failing jet temperature registrations (thermometer reached its bottom limit).

degrees of subcooling by using the two-phase model suggested in this work (See the Appendix). The reasons for this are as follows:

- The model predicts accurately the outlet pressure (Figs. 5 and 6) and the

Fig. 11. Icy ground deposits after a release.

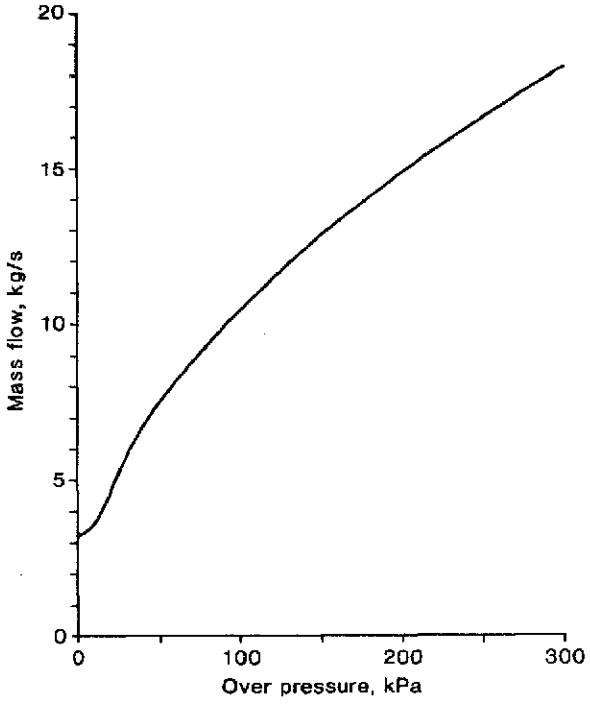

Fig. 12. Calculated (See the Appendix, model 1) mass flow rate against overpressure for the pipe releases in these field tests

average discharge rates (Table 1) in our experiments with markedly subcooled sulfur dioxide.

- The same model predicts accurately the mass flow rates in the analogous experiments [1] with saturated ammonia.

We therefore believe that this model is capable of explaining how mass flow rate varies with the tank liquid overpressure. Figure 12 illustrates calculated mass flow rates for a tank liquid temperature and a release geometry corresponding to trial P3. (The curve is approximately valid for the other pipe releases as well.) Notice that the mass flow rate is very sensitive to changes in the excess pressure, e.g. in trial P3 the initial overpressure was 260 kPa which gives a calculated mass flow rate 17 kg/s. This is to be compared with 3.2 kg/s which is the result without overpressure. Hence the subcooling of the tank liquid is not a negligible factor as regards possible hazards.

Another important aspect is how subcooling influences the entrainment of air into the jet if an inflammable gas is released through a channel configuration. The air entrainment is mainly caused by the momentum flow rate of the jet which is given by (let us neglect gravitation and wind to begin with)

$$F = gu_e + A(P_e - P_a) \tag{4.1}$$

The second term in this equation is mostly much larger than the first term and furthermore it tends to remain almost constant when the overpressure is varied. This means that the momentum flow rate varies less than the mass flow rate.

Let us again compare the model calculations (Fig. 12) mentioned above to get a concrete example.

At an overpressure of 260 kPa (corresponding to the beginning of trial P3) we obtain that $g=17$ kg/s, $u_e=12.0$ m/s, $P_e=300$ kPa and hence that $F=408$ N. With no overpressure we obtain that $g=3.2$ kg/s, $u_e=9.8$ m/s, $P_e=253$ kPa and that $F=188$ N.In other words, the momentum flow rate increases far less than the mass flow rate if the vessel pressure is raised above the saturation pressure. The consequence of this is that the ratio of velocity to concentration in the jet becomes smaller if the tank liquid is overpressurized. This means that the transition from a momentum jet dispersion state to a state dominated by atmospheric motion and gravitation occurs at higher concentrations. Consequently, the probability for the formation of large flammable clouds increases.

4.2 The influence of release geometry

We have already concluded that release of pressurized liquefied gas through a duct could mean a considerable reduction of the mass flow rate. This is due to the flash of superheated liquid in the duct. Moreover, the high exhaust pressure causes the discharge speed (just before air mixes with the gas) to increase substantially. This increases the initial air entrainment and reduces the fire risks in cases where the gas is inflammable.

On the other hand it was also concluded that much of these advantages could be lost if the vessel pressure is higher than the saturation pressure of the liquid, since the mass flow rate increases rapidly with overpressure.

If a tank is perforated or if the gas is released through some kind of short channel a disadvantagous situation occurs. Our tests show that the fluid remains a pure liquid all the way up to the exit orifice. Moreover, it appeared that (within the accuracy of the measurements) the exit pressure was not higher than the atmospheric back pressure. Firstly, this means that the mass flow rate becomes the maximum possible (Bernoulli's liquid flow equation is valid) from the physical point of view. Secondly, the substance achieves no acceleration outside the hole when the fluid expands. Thus the axial speeds in the jet become as small as possible compared to its concentrations. This of course enhances the possibility for flammable cloud formation as atmospheric motion and gravity may take over the spreading at high concentrations.

4.3 Temperatures and ground deposits

As mentioned earlier the temperature was considerably lower than the atmospheric boiling point already at 2 m distance from the release orifice along the jet axis. This shows that a substantial amount of air has reached the jet axis

already at that place. This is in fact not surprising when considering the initial rapid widening of the jet diameter.

Let us assume a complete flash to take place immediately after the orifice and that no air is allowed to mix with the jet. By using the experimental mass- and momentum flow rates we find that the initial jet diameter (when atmospheric pressure is reached) should become smaller than 20 cm in all our trials. This is to be compared with the actual initial diameters of about 1 m. The conclusion is that the radial momentum produced by the flash causes an extra air entrainment allowing for a considerable evaporation of the liquid phase very near the exhaust hole.

The temperature where the jet impinged on the ground immediately reached values far below the atmospheric boiling point. Despite this no liquid deposits of sulfur dioxide formed at all. Not even the release P1, where more than 400 kg were released during 40 s, showed any signs of liquid pools. The ground deposits consisted only of a thin layer of condensed water vapour in the form of white frost.

Let us first consider the possibility that there are droplets in the cloud when it reaches the ground but that they do not impact. This is only possible when the diameter of the aerosol particles is about 0.1–1 μm [2] in which range the penetration through the laminar sublayer is prevented. This size is far smaller than the drop sizes (10–100 μm) obtained by Brown and York [3] in laboratory experiments with flashing water and freon at higher vessel pressures than ours. Therefore, it is reasonable to conclude that the liquid phase is completely or almost completely evaporated when it reaches the ground.

This is far from impossible if it is accepted that the air–sulfur dioxide mixture approaches equilibrium almost instantaneously. If (at atmospheric pressure) the substance released in our tests (quality factor 10%, temperature $-10°C$) is mixed with the air (about 17°C and 70% relative humidity), a simple enthalpy balance yields that an air mass fraction of only 69% is sufficient for a complete evaporation. Such a calculation also gives the minimum possible temperature which is $-43°C$.

5 Conclusions

Releases of condensed sulfur dioxide at 15–20°C from the liquid space of a pressure vessel through a pipe and through an aperture have led to the following conclusions:

(a) A pipe (or some other similar configuration) does not necessarily reduce the mass flow rate significantly through the mechanism of flash in the release channel. Even a moderate subcooling (i.e. the pressure is higher than the saturation pressure) may destroy this favourable effect and cause a much larger mass flow. Therefore, steps to avoid subcooling of the vessel liquid could sometimes be useful for hazard reduction.

(b) Release from the liquid phase through a hole directly in the tank wall (or a short channel) does not seem to be associated with any physical mechanisms reducing the hazards. The gas remains a liquid all the way up to the exhaust hole and the exit pressure is not higher than the atmospheric back pressure. This gives a maximum possible mass flow rate and an unfavourable initial air entrainment.

(c) Conventional bunds surrounding pressure vessels might be of limited value. Not even the low thermodynamic pressure energy of sulfur dioxide at moderate summer temperatures allowed any liquid ground deposits at all. The liquid phase formed an aerosol which evaporated almost instantaneously with no liquid accumulation on the ground although the distance from the release point to the nearest point of ground contact was not more than 2 m. One of the mechanisms making this quick evaporation possible is the extra air entrainment caused by the rapid radial expansion (due to flashing) just outside the exhaust hole.

(d) The rapid evaporation causes the temperatures to become very low near the release hole. This may complicate manual steps against an accidental release as the protective suits must resist low temperatures.

(e) The mathematical models presented in this work seem to be reliable tools in assessing the essential physical quantities (mass flow rate and some of the jet determining parameters) when a toxic or inflammable gas is released from a pressure vessel.

(f) Further efforts are needed to find out how air is mixed into a spray jet formed by a flashing liquid. It is also necessary to investigate how the ground (or other obstacles) affects the air entrainment and consequently the possible fire hazards.

Acknowledgements

The authors wish to acknowledge the personnel at the safety department of the Boliden Metall Co. whose professional skills made this work possible. We are specially grateful to Mr. Å. Nygren, Mr. G. Lundmark, and Mr. G. Karlsson for designing and constructing the ingenious equipment making repeated "hole in the tank wall"-tests possible in a safe way. We also wish to thank Mr. L. Svensson, Mr. M. Nordstrand, and Miss M. Fjaellström at our institute for their invaluable participation. This research was financially supported by the Boliden Metall Co., the Boliden Kemi Co., and the Swedish Fire Research Board.

List of symbols

A	Cross sectional area of pipe or aperture throat
C_D	Coefficient of contraction for liquid flow into a tube

D	Inner diameter of the pipe
e	Equivalent sand roughness number
F	Momentum flow rate (of turbulent jet)
g	Mass flow rate
h_{sat}	Heat of vaporization at saturated conditions
L	Pipe length
P_a	Atmospheric pressure
P_e	Exit pressure (pipe end or aperture throat)
P_o	Tank pressure
R	$D/2$
S_l (P, T)	Liquid entropy at pressure P and temperature T
$S_{l, sat}$	Liquid entropy at saturated conditions
T_o	Temperature of the tank liquid
T_{sat}	Temperature at saturated conditions
u_e	Velocity (of two-phase fluid) at pipe end
V_e	Specific volume (of two-phase fluid) at the pipe end
$V_{g, sat}$	Specific volume of the vapour at saturated conditions
V_l	Specific volume of the liquid phase
x_e	Weight fraction (quality) of vapour at the pipe end
α	Volume ratio parameter = Average specific volume (along the whole length of the duct) to exit specific volume for the pipe fluid (equal to 1.0 in this work)
λ	Friction factor (pipe wall)
ζ	Pressure loss coefficient for the pipe inlet

References

1 K. Nyren and S. Winter, Two phase discharge of liquefied gases through pipes. Field experiments with ammonia and theoretical model, In: 4th Int. Symp. on Loss Prevention and Safety Promotion in the Process Industries, Harrogate, 1983, Pergamon Press.

2 C. Persson and G. Omstedt, A model for calculation of dispersion and deposition of air pollution in mesoscale, SMHI Rapporter, no. RMK 20, 1980.

3 R. Brown and J.L. York, Sprays formed by flashing liquid jets, AIChE J., 8 (1962) 149–153.

4 B. Fletcher, Discharge of saturated liquids through pipes, J. Hazardous Materials, 8 (1984) 377–380.

5 H. Rouse, Elementary Mechanics of Fluids, Dover Publications, New York, 1978, p. 205.

6 R.B. Bird, W.E. Stewart and E.N. Lightfoot, Transport Phenomena, John Wiley & Sons, New York, 1960, p. 217.

7 G. Seger and H. Cramer, Die termischen Eigenschaften der schwefligen Säure nach neuesten Versuchen, Z. Kälte-Ind., 46 (1939) 183–184.

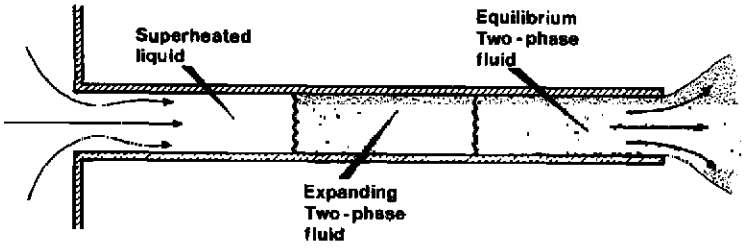

Fig. 13.

Appendix

Theoretical models used to interpret the results

1 Two-phase release through a pipe. Model 1

The model is almost the same as the one suggested in Ref. [1] where postulates and derivations are dealt with in detail. Figure 13 illustrates the essential principles and shows how a delayed adiabatic flash is supposed to occur in the pipe. The original version [1] was slightly modified inasmuch as the rapid evaporation in the pipe entrance was replaced with an assumption that the flash is more delayed (see Fig. 13). This assumption means that model 2 (see below) can be used to treat the liquid flow up to the point where the flashing starts. From this point up to the pipe end the flow of the expanding two-phase fluid is treated in the same way as in Ref. [1].

This change in the postulate system has no influence as long as the tank liquid is close to its boiling point (phase equilibrium). On the other hand the new approach works better if the tank liquid is subcooled, which was the case in all trials in this work. The model for instance predicts a one-phase (liquid) flow in the whole pipe if the degree of subcooling is large enough; a flow condition which the original model [1] was not designed to cope with in a physically correct manner. The new assumption, however, makes the model capable of dealing with virtually any kind of non-equilibrium in the tank.

Following the procedure in Ref. [1], the mass flow rate g becomes a unique function of the exit pressure P_e

$$g(P_e) = A\left(\frac{P_o - P_e}{V_e(1+L\lambda\alpha/2D) - (V_l/2)(1-\zeta)}\right)^{1/2} \tag{A.1}$$

(Notice that this equation is not entirely identical to the corresponding equation in Ref. [1] because of the different treatment of the flow entry.) The mass flow rate and the critical exit pressure is then obtained from eqn. (A.1) by maximizing the function $g(P_e)$.

The exit specific volume V_e of the two-phase fluid is

$$V_e = x_e V_{g,\,sat}(P_e) + (1-x_e)V_l \tag{A.2}$$

where the exit quality factor is

$$x_e = \frac{T_{sat}(P_e)}{h_{sat}(P_e)} \left[S_l(P_o, T_o) - S_{l,\,sat}\,(P_e) \right] \tag{A.3}$$

This is the model design as it has been used in this work (where the geometrical circumstances are very simple). If the release pipe system is more complex (pipe bends, valves, etc.) it is recommended to replace the factor multiplying V_e in eqn. (A.1) with the alternative expression suggested in Ref. [1]. When evaluating the pipe experiments in this work complete equilibrium at the pipe end was assumed and appeared to give a good fit. Other experiments in the literature [4] also support an equilibrium assumption.

For the friction parameter it has been assumed that the equation [5]

$$\frac{1}{\sqrt{\lambda}} = 2\ {}^{10}\log(R/e) + 1.74 \tag{A.4}$$

is valid because the Reynold's numbers in our experiments exceeded 10^6 and R/e was 400. The pressure-loss coefficient ζ for the pipe inlet was chosen to be 0.45 in accordance with Ref. [6].

The thermodynamic state functions in eqns. (A.2) and (A.3) have not been replaced with simple correlations but instead (in order to avoid unnecessary errors) experimental data [7] for saturated sulfur dioxide have been used.

Since the tank liquid is almost incompressible it was assumed that the entropy of the subcooled liquid could be represented by

$$S_l(P_o, T_o) = S_{l,\,sat}(T_o) \tag{A.5}$$

The model predicts an interesting flow state when the tank liquid is subcooled. Figure 14 illustrates what happens when the exit pressure P_e in eqn. (A.1) is varied in four different cases all having the same tank temperature but different tank pressures. The lowest curve corresponds to saturated equilibrium in the tank while the others correspond to a subcooled (overpressurized) tank liquid. The dots 1–4 mark the maximum points where the flow parameters are postulated to settle in steady flow. Note that if the tank pressure exceeds a certain threshold value we obtain a critical flow state where the critical exit pressure equals the saturation pressure of the liquid independent of the vessel pressure. The fluid is then a liquid in the entire release channel. Also notice the marked increase in the discharge rate already at moderate overpressures.

2 Liquid release through a pipe, Model 2

This model was used to decide whether the experimental pipe flows were liquid or two phase flows. The use of a simple mechanical energy balance for an incompressible fluid gives

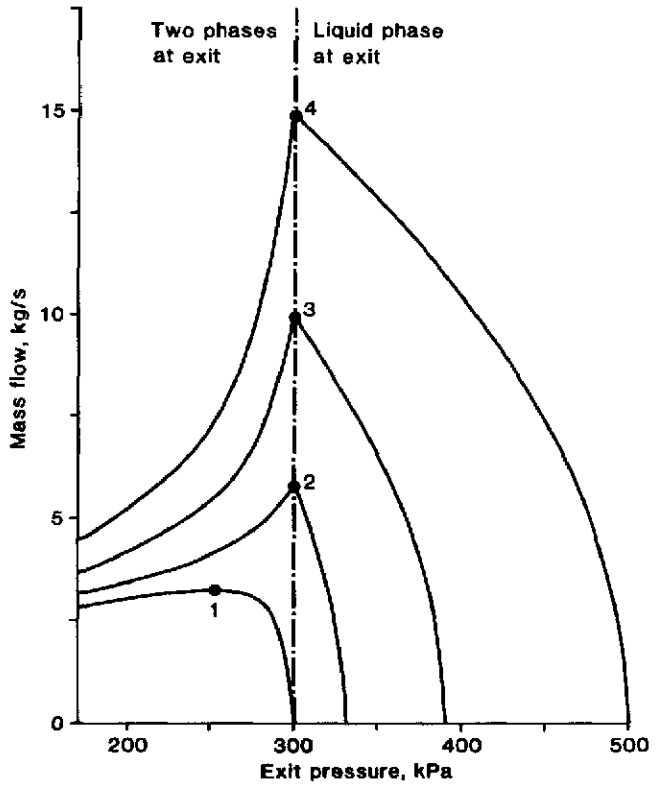

Fig. 14. Example (sulfur dioxide with the pipe geometry shown in Fig. 2) showing typical results of varying the exit pressure in eqn. (A.1). Four cases with the same tank liquid temperature (17.2°C) but different tank pressures (300, 330, 390, and 500 kPa, respectively) are shown. The dots 1–4 are the maximum points corresponding to steady state critical flow.

$$g = A\left(\frac{2(P_o - P_e)}{V_i(1 + L\lambda/D + \zeta)}\right)^{1/2} \tag{A.6}$$

The short wide channel (see Fig. 2) before the pipe is not taken into account in this equation because it affects the mass flow rate negligibly. Another thing to be pointed out is that eqn. (A.1) transforms into eqn. (A.6) if the exit volume is set equal to the liquid phase volume, i.e. eqn. (A.6) is a special case of eqn. (A.1). The parameters ζ and λ have the same values as in the previous section.

3 Liquid release through an aperture. Model 3

The same simple arguments (but with neglect of wall friction) as in the previous section gives

$$g = C_D A \left(\frac{2(P_o - P_e)}{V_l} \right)^{1/2} \tag{A.7}$$

The coefficient of contraction C_D was chosen to be 0.50 because of the geometrical resemblance to a short reentrant pipe (see Fig. 2).